Journal of Renewable Materials

Tech Science Press

Doi:10.32604/jrm.2025.02024-0068

ARTICLE

Grafting Modification of Cellulose Nanofibril with 2-(N,N-Dimethylamino) Ethyl Methacrylate and 2-Hydroxyethyl Methacrylate as a Barrier-Improved Coating for Paper-Based Food Packaging

Noverra Mardhatillah Nizardo[1,*], Alifah Nurul Saffanah[1], Annisa Fitri Salsabila[1], Amanda Aurellia Putri[1], Aniek Sri Handayani[2], Azizah Intan Pangesty[3] and Mochamad Chalid[3]

[1]Department of Chemistry, Faculty of Mathematics and Natural Sciences, Universitas Indonesia, Depok, 16424, Indonesia
[2]Department of Chemical Engineering, Institut Teknologi Indonesia, Tangerang Selatan, 15314, Indonesia
[3]Department of Metallurgical and Material Engineering, Faculty of Engineering, Universitas Indonesia, Depok, 16424, Indonesia

*Corresponding Author: Noverra Mardhatillah Nizardo. Email: noverra.mardhatillah@sci.ui.ac.id

Received: 21 December 2024; Accepted: 28 April 2025; Published: 23 June 2025

ABSTRACT: Food packaging is becoming popular as the consumption of ready-to-eat food products rises. Easy-to-use, non-biodegradable plastic packaging is commonly used in food packaging, contributing to the deteriorating environmental situation. This issue increases the concern for the environment and encourages the usage of alternative materials. Cellulose nanofibrils (CNF) are abundant and biodegradable, which makes them ideal candidates to replace plastic coatings. The ability to form H-bonds between the hydroxyl groups makes coated paper with CNF have good strength, but poor barrier properties. The barrier properties can be improved by grafting DMAEMA or HEMA onto CNF (CNF-g-PDMAEMA and CNF-g-PHEMA, respectively). Thus, the objective of this study was to modify CNF chemically to enhance the barrier properties of the food packaging paper. It was found that paper coated with CNF-g-PDMAEMA and CNF-g-PHEMA exhibited improvements in mechanical and barrier properties while maintaining the desired viscosity for the coating process. The water contact angle increased for paper coated with CNF-g-PHEMA and CNF-g-PDMAEMA, reaching a maximum of 97.51° and 92.58°, respectively with the decreasing $Cobb_{60}$ values by 49% and 11%. The oil absorption was also reduced for both coated papers compared to the blank paper. Mechanical properties improved, as indicated by a 3% increase in tensile strength for paper coated with CNF-g-PHEMA and a 5% for paper coated with CNF-g-PDMAEMA. The results indicated significant potential for the application of modified CNF in coatings for food packaging paper. Noteworthy, the grafting process should be improved to enhance the mechanical and barrier properties of the coated paper.

KEYWORDS: Cellulose nanofibril; grafting; biopolymer modification; paper coating; barrier properties

1 Introduction

Packaging is a major component in maintaining and protecting product quality from exposure to microorganisms or other contaminants [1]. Polymers currently widely used in the packaging industry come from petroleum derivatives [2]. Unfortunately, petroleum-based synthetic polymers often used in the packaging industry today are not easily biodegradable. Therefore, they are not environmentally friendly and can cause pollutants [3]. Moreover, excessive use of plastic-based packaging can cause environmental pollution due to raw plastic materials that are not degradable [4].

The production of plastic as food packaging has increased significantly, but only about 9% of the 6300 metric tons of plastic made in 2015 has been recycled, 12% incinerated, and the rest accumulated in the environment. In this case, it is estimated that there will be 12,000 metric tons of plastic accumulated globally by 2050 [5]. Therefore, alternative raw materials that are more environmentally friendly are needed to prevent damage to the earth. One promising solution for packaging material is by using biopolymers which are produced from natural sources, i.e., cellulose [6], due to their wide availability in nature [7,8], good stability, structure, biocompatibility, and biodegradability [9]. However, most paper packaging might experience food spoilage because of water from humidity, oil from the food itself, and oxygen transmission from the air. In addition, paper packaging has poor mechanical properties. To improve the barrier and mechanical properties of paper, a coating is needed [10]. Generally, a coating for paper-based packaging originates from plastic. Nonetheless, along with increasing concern for the environment, sustainability must be considered.

Cellulose nanofibrils (CNF) have been developed as an alternative material to form a coating layer. This type of nanocellulose is a futuristic material because it has high crystallinity, good mechanical resistance, optical transparency, polyfunctionality, hydrophilicity, and a high specific surface area [9]. Nonetheless, CNF also has a disadvantage as it has many hydroxyl groups on the surface causing it to be hydrophilic and could not retain water [11]. Therefore, a modification of CNF is needed to optimize the water and oil resistance of CNF coating. Cellulose can be blended with various polymers to increase the mechanical properties as a food packaging paper [8].

CNF modification can generally be divided into two types, namely physical and chemical modification [12]. Physical modification can be done through adsorption, and this method is relatively easy because it does not require a new covalent bond formation reaction and can use water as a medium. This adsorption can be done by adding other polymers, such as ionic polymers, such as poly(ethylene imine) (PEI) [13], and nonionic polymers, for example, poly(ethylene glycol) (PEG) [14], poly(vinyl alcohol) (PVA) [15], and carboxymethyl cellulose (CMC) [16]. Despite having the advantages mentioned above, physical modification also has disadvantages, namely, the absence of chemical bonds so that leaching can occur [12].

Meanwhile, chemical modification can occur through reactions between OH groups on CNF with other molecules using grafting methods. Grafting methods consist of molecular grafting, for example with esterification or acetylation reactions using small molecules on OH groups in CNF, or polymer grafting, namely by reacting groups in polymers with OH groups in CNF. An example of polymer grafting is by reacting PEG with TEMPO-oxidized CNF so that the PEG chain will form an ester [17]. The grafting method is widely used due to the ability to combine two or more desired monomers in one polymer [18].

Littunen et al. modified CNF through a grafting method using a catalyst to tailor CNF hydrophobicity. This research carried out a comparison of CNF modification with various acrylate and methacrylate monomers. Synthesis of graft copolymers was carried out using the free radical polymerization method using ammonium cerium (IV) nitrate catalyst. This method has proven to be efficient and selective and produces products which are dominated by graft copolymers compared to homopolymers. The results showed that modification of CNF with acrylate and methacrylate monomers used succeeded in increasing the hydrophobicity of CNF [19].

Kedzior et al. also reported the results of their research regarding surface grafting of cellulose nanocrystals (CNC) with poly(methyl methacrylate) (PMMA) using the free radical polymerization method to overcome its high hydrophilicity and low thermal stability. The results obtained stated that there was a twofold increase in the water contact angle of the modified CNC. Therefore, it can be concluded that there had been an increase in hydrophobicity properties [20].

Hollertz et al. studied chemically modified cellulose micro and cellulose nanofibrils and successfully used them as paper-strength additives. Three different types of cellulose nanofibrils (CNFs) were investigated, namely carboxymethylated CNFs, periodate-oxidized carboxymethylated CNFs, and dopamine-grafted carboxymethylated CNFs. These CNFs showed a strong tendency to form films around the fibers and significantly improved the mechanical properties of the sheets [21].

The incorporation of CNF as a coating material into paper might increase tensile strength, reduce its porosity, and improve density [22]. A huge improvement in barrier properties (oxygen permeability, oil resistance, and moisture resistance) when paper was coated with a thin layer of microfibrillated cellulose (MFC) using a rod coater for sheets was reported [22,23]. Nevertheless, in packaging applications, CNF films did not show the desirable effect on improving the water barrier property of paper. The CNFs have a high specific surface area and plentiful surface hydroxyl groups, so they have high hydrophilicity and affinity with water [24]. In this case, the work about laminate barrier with a layer of CNF modified with polymer providing hydrophobicity was reported as a good combination for optimal function [25]. In addition, Garcia-Valdez et al. reported that DMAEMA-modified cellulose nanocrystal (CNC) provided the CNCs with increased hydrophobicity [26].

Coating technology is a promising solution to enrich the shortcomings of biobased polymers particularly the barrier properties [27]. There are various coating techniques including chemical/physical vacuum deposition, solution coating (e.g., layer-by-layer assembly, slot-die coating, spray coating, spin coating, and dipping), electrohydro-dynamic processing (e.g., electrospraying, electrospinning) and other techniques such as bar/rod-coating, melt extrusion coating and hot pressing [28]. Bar/rod-coating represents a non-solvent technique, eliminating issues related to solvent use. This method offers improved control over coating thickness [29] determined by the size of the groove or notch on the bar and is relatively simple and cost-effective [30].

Most of the current research has primarily focused on studying the reaction to prepare CNF-graft copolymers. To the best of our knowledge, there has been relatively limited research on the use of CNF-graft copolymers as a coating on paper packaging and investigating their barrier properties. Thus, we tried to fill this research gap by reporting our findings. By using this method of grafting, the binding between cellulose and corresponding monomers could be stronger. This binding might enhance the interaction between paper as the substrate and the graft copolymer itself as the coating material through the H-bonds that come from the hydroxyl group of the cellulose chains in the paper as well as in the graft copolymer. In addition, the barrier properties of CNFs could be improved by a grafting modification that would transform the hydroxyl group into an ester group. This led to the increasing hydrophobicity of CNF and decreasing water absorption of paper. Moreover, due to the filling porosities and increased mechanical entanglements between fibrils with an increased number of inter-fiber bonds, the mechanical strengths and the oxygen permeability of the grafted CNF paper were enhanced. Thus, this research focused on the chemical modification of CNF that was carried out using redox-initiated free radical copolymerization using 2-(N,N-dimethylamino)ethyl methacrylate and 2-hydroxyethyl methacrylate as a coating for paper-based food packaging. The grafting process was carried out by varying the reaction time, initiator concentration, and monomer amount to determine which graft copolymer produces the best degree of grafting (DoG). The graft copolymers were then characterized using Fourier transform infrared (FTIR) to analyze functional groups. Afterwards, graft copolymers were applied to paper as a coating. Then, the performance of paper coated with graft copolymers was tested using a water vapor transmission rate (WVTR) test, water contact angle test, water absorption test, oil absorption test, and tensile strength test.

2 Materials and Methods

2.1 Materials

Oil palm empty fruit bunches (OPEFB) were obtained from Sulawesi, Indonesia. Ceric ammonium nitrate (CAN purity of 98.5%, irritant and corrosive, flammable, LD_{50} = 300–2000 mg/kg), 2-(N,N-dimethylamino) ethyl methacrylate (DMAEMA purity of 98%, irritant and corrosive. LD_{50} = 1751 mg/kg), and 2-hydroxyethyl methacrylate (HEMA purity of 99%, irritant. LD_{50} = 5564 mg/kg) were purchased from Sigma Aldrich. Nitric acid (corrosive, acute toxicity) was purchased from Merck. Acetone (irritant and flammable. LD_{50} = 20,000 mg/kg), ethanol (irritant and flammable. LD_{50} = 10,470 mg/kg), methanol (carcinogenic, flammable, and acute toxicity. LC_{50} = 15,400 mg/L), diethyl ether (flammable and irritant. LD_{50} = 1211 mg/kg), and (THF carcinogenic, irritant, and flammable. LD_{50} = 1651 mg/kg) were purchased from Smart Lab. All chemicals were used as received.

2.2 Synthesis of Microfibrillated Cellulose (MFC)

MFC was produced from OPEFB through a chemical method known as the multi-step bleaching process, as demonstrated in research by Septevani et al. [31]. The synthesis started by soaking the OPEFB for 24 h in distilled water and acetone. Then, the OPEFB was dried in an oven, and the particle size was reduced using a Fomac machine and a 100-mesh sieve. Next, 150 g of sieved OPEFB was mixed with NaOH solution of 4 wt% on a hot plate at 80°C for 3 h, followed by washing and filtering until the neutral pH was achieved. This process was repeated three times. The OPEFB was then bleached by mixing it with an acetate buffer solution (40.5 g of NaOH, 112.5 mL of glacial acetic acid, and 1500 mL of H_2O) on a hot plate at 80°C for 2 h, followed by washing and filtering until the pH was neutral. Afterward, the OPEFB was mixed with a 1.7% $NaClO_2$ solution at 80°C for 2 h, followed by washing and filtering until obtaining a neutral pH. This bleaching process was repeated for a total of three cycles. Finally, the OPEFB was dried in an oven at 40°C for 36 h.

2.3 Synthesis of CNF

CNF 2% was prepared from MFC using a mechanical homogenization method based on research by Nizardo et al. [16]. To achieve a 2% concentration, 40 g of MFC was added to 1960 mL of distilled water and was stirred with an Ultraturrax (Staufen, Germany) for 8 h at 20,000 rpm, with a cycle of 10 min on and 10 min off. Subsequently, the MFC was sonicated using an ultrasonic Hielscher (Teltow, Germany) for 5 min, with a cycle of 10 s on and 10 s off. The total sonication time was 90 min.

2.4 Graft Copolymerization

The synthesis procedure for graft copolymerization was carried out using the method developed by Littunen et al. [19]. CNF suspension with a concentration of 2 wt% was placed into a three-necked flask, and its pH was adjusted to 1 by adding nitric acid. After that, nitrogen gas was passed through the solution. After 15 min of stirring, ammonium cerium (IV) nitrate (CAN) catalyst was added to the mixture. The mixture was stirred again for 15 min while being heated to 35°C. The monomer was gradually added over 30 min, and the mixture was stirred again for 30 to 120 min. Next, the mixture was centrifuged, and the precipitation was washed with water to remove the catalyst and acid. The precipitate was then washed with acetone and THF for CNF-g-PDMAEMA, and methanol for CNF-g-PHEMA, to separate the homopolymer from the graft copolymer. The resulting product was dried overnight at room temperature. Variations in reaction time, CAN concentration, and number of monomer moles are displayed in Table 1.

Table 1: Recipe for the synthesis of graft copolymers

Sample	CNF 2% (mL)	Time (min)	CAN (mM)	Monomer (mmol)
CNF-g-PDMAEMA 1	50	30	5	20
CNF-g-PDMAEMA 2	50	60	5	20
CNF-g-PDMAEMA 3	50	90	5	20
CNF-g-PDMAEMA 4	50	120	5	20
CNF-g-PDMAEMA 5	50	90	3	20
CNF-g-PDMAEMA 6	50	90	7	20
CNF-g-PDMAEMA 7	50	90	7	10
CNF-g-PDMAEMA 8	50	90	7	30
CNF-g-PHEMA 1	50	30	3	20
CNF-g-PHEMA 2	50	60	3	20
CNF-g-PHEMA 3	50	90	3	20
CNF-g-PHEMA 4	50	120	3	20
CNF-g-PHEMA 5	50	60	1	20
CNF-g-PHEMA 6	50	60	5	20
CNF-g-PHEMA 7	50	60	5	10
CNF-g-PHEMA 8	50	60	5	30

2.5 Characterization of Graft Copolymers

The results of graft copolymerization synthesis were characterized by FTIR to investigate the new peaks of functional groups formed from the grafting process and determine the DoG. Determination of the DoG was performed by calculating the magnitude of transmittance at the wavenumber of the C=O carbonyl region of the product and monomer, as shown in Eq. (1).

$$\text{Degree of grafting} = \frac{\text{T of C = O in product}}{\text{T of monomer}} \times 100\% \quad (1)$$

NMR characterization was also carried out to determine the chemical composition of the graft copolymers formed. Graft copolymers were also tested for their viscosity to determine the coating ability when used to coat paper using the bar coater method. Viscosity measurements were carried out using a Brookfield viscometer. XRD characterization was conducted using XRD Aeris (Malvern Panalytical, Malvern, UK) using Cu Kα radiation with scattered radiation detected in the range of 5–95°. Furthermore, the crystallinity index by XRD (CI_{XRD}) value was measured to quantify the crystallinity of the graft copolymers [32], as shown in Eq. (2).

$$CI_{XRD} = [(IC - IA)/IC] \times 100 \quad (2)$$

where *IC* and *IA* represent the maximum peak intensity corresponding to the crystalline region at 2θ 22° and the amorphous region at 2θ 16°, respectively.

2.6 Coating Process

The coating process using the bar coating method was carried out based on the research of Nizardo et al. with slight modifications [16]. The solutions of CNF-g-PDMAEMA and CNF-g-PHEMA were prepared before the coating process. Subsequently, CNF-g-PDMAEMA and CNF-g-PHEMA were dissolved in

methanol and ethanol, respectively, in a ratio of 1:3. In the bar coater machine, the paper was clamped, and then the bar coater was installed. Next, the solutions of graft copolymers were poured onto the paper, and the machine was run at a speed of 50 mm/s for one pass until the coating was evenly distributed. The initial coating process was carried out using different bar coater sizes: 4, 6, 8, 25, and 60 μm. The paper was then dried on a hot plate until completely dry.

2.7 Performance of Graft Copolymers Coating on Packaging Paper

The coated paper was tested through several methods to see its performance as packaging. The water absorption of the coated paper was tested using the $Cobb_{60}$ method based on ISO 535. This method calculates the amount of water absorbed into the paper over 60 s, with 45 s of contact time between the water and the paper, and the remaining 15 s used to remove excess water by rolling with an iron cylinder. In the case of the water contact angle, water was dripped onto the coated paper, and the angle formed on the paper was then measured. Furthermore, the water vapor resistance of coated paper was tested by a water vapor transmission rate (WVTR) test. This method measured how much water vapor was blocked by the graft copolymer-coated paper. The oil absorption test was studied using the IGT method which complies with the SNI 14-0584-1989 standard, in which the concept was to observe the amount of oil absorbed into the paper, indicated by the length of the oval stain that appears on the paper sheet. Finally, a tensile strength test was performed by clamping the paper sample in the instrument holder, and the machine pulled the paper until it tore. The number displayed after the paper tears was the tensile strength.

3 Results and Discussion

3.1 Synthesis of MFC and CNF

MFC was synthesized from the oil palm empty fruit brunch OPEFB through pretreatment alkali and bleaching treatment. Cellulose nanofibril (CNF) can be obtained from the oil palm empty fruit bunches (OPEFB) waste. OPEFB constitutes approximately 20%–30% of the total weight of fresh palm fruit, contains a significant cellulose content for about 30%–40% of its dry weight [33]. OPEFB waste, as a source of cellulose, offers a solution for managing the abundant OPEFB waste generated in Indonesia [34]. Some researchers have utilized OPEFB waste as the source of cellulose [34–36]. Alkali treatment was used to remove alkali-soluble compounds such as lignin and hemicellulose while bleaching treatment was carried out to break phenolic compounds and side products [37]. The change in color of the fiber after alkali and bleaching treatment was related to the degradation of lignin and hemicellulose [37]. Bleaching under acidic pH conditions—achieved in this study through the use of an acetate buffer—promoted the opening of the fiber and cell wall structure, especially the outer layer in the form of a wax layer, and induced partial depolymerization. This process could significantly improve the removal efficiency of hemicellulose and lignin [38]. Lignin and hemicellulose must be removed because they could reduce the brightness and mechanical properties of cellulose [39,40]. The pretreatment step of removing hemicellulose and lignin was aimed at producing cellulose with a high degree of purity and reduced crystallinity [41]. After all, the resistance of individual fibers was decreasing. MFC was then processed through ultraturrax and ultrasonic to reduce fiber particle size into nano utilizing mechanical shear force [18]. The process was followed by ultrasonication, in which cellulose pulp was exposed to sonic waves to homogenize the suspension [11]. Product CNF 2% was synthesized with a mass percentage of 2.05% with an average particle size of 231.7 nm and polydispersity index of 0.599. These results were similar to the PSA results from the study of Radakisnin et al. [42].

3.2 Graft Copolymerization

3.2.1 FTIR Characterization

FTIR characterization was carried out for CNF, DMAEMA, HEMA, CNF-g-PDMAEMA, and CNF-g-PHEMA, which is shown in Fig. 1. The graft copolymerization product showed a new peak of absorbance band at 1710–1740 cm^{-1}. This indicated that the graft copolymers were successfully formed because the peak represented the characteristic of the ester carbonyl group [43]. There was also a broad and strong absorption peak at 3300 cm^{-1} of hydroxyl group from CNF. According to previous work of Credou [44], hydroxyl groups in glucose units were responsible for cellulose chemical activity. Other peaks found were CH stretching peaks at 2850–2900 cm^{-1}. Ester carbonyl group peaks on CNF-g-PDMAEMA appeared in the range of 1718–1720 cm^{-1} while for CNF-g-PHEMA appeared in the range of 1720–1740 cm^{-1}.

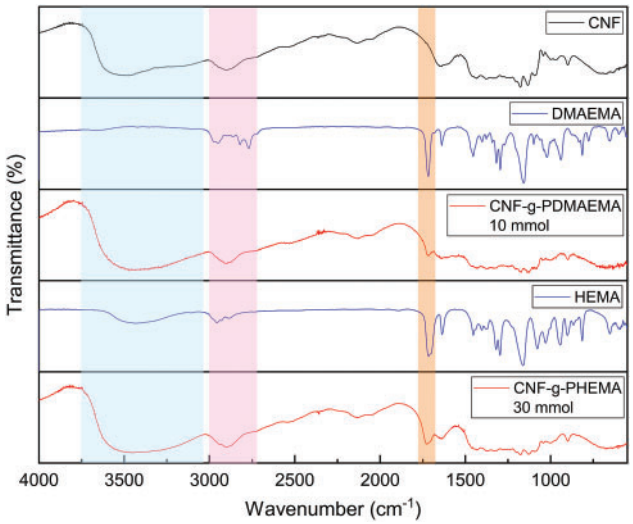

Figure 1: FTIR spectra of CNF, DMAEMA, CNF-g-PDMAEMA, HEMA, and CNF-g-PHEMA

3.2.2 NMR Characterization

NMR spectroscopy was conducted to determine the chemical composition of graft copolymer. Fig. 2 displays the ^{1}H-NMR spectrum of CNF-g-PDMAEMA. Cellulose proton gave a signal at 4–6 ppm. The peak at 2.5 and 3.3 ppm resulted from DMSO and H_2O, respectively. The peak of H_1 of the DMAEMA methyl group appeared at 1.8 ppm, while the peak of H_2 secondary alkyl appeared at 2.27 ppm. Protons of H_3, H_4, and H_5 of DMAEMA were experiencing a deshielding effect that resulted in peak shifting into downfield. Hence, the peak emerged at 3.6, 2.9, and 2.64 ppm, respectively. These results are in good agreement with the reference ^{1}H-NMR spectrum from the research of Liu et al. regarding lignin-graft-PDMAEMA [45].

A ^{13}C-NMR spectrum of CNF-g-PDMAEMA is shown in Fig. 3. The presence of peaks at 18.45 and 18.55 ppm showed the existence of carbon of methyl group C_3, C_7, and C_8 of DMAEMA. An overlapping peak was found at 43.65 ppm which corresponded to alkyl group C_1 and C_2 DMAEMA. Peaks belonging to C_6, C_5 of DMAEMA, and C_6 of cellulose were also overlapping at 45.45 ppm. Their peaks were overlapping because both are secondary alkyl groups that were located next to electronegative atoms (oxygen and nitrogen). Furthermore, peaks at 56.31 ppm ensured the existence of C_2, C_3, and C_5 of cellulose. In addition, peaks at 57.34 and 59.44 ppm belonged to C_4 and C_1 of cellulose. However, the peak of C_4 of DMAEMA, which should be at 120 ppm, did not appear because the DoG of CNF-g-DMAEMA was small enough indicating the C=O

carbonyl group was very small in the product. The resulting ^{13}C-NMR spectrum was in accordance with the ^{13}C-NMR spectrum from research by Neelamegan et al. [46], research by Okushita et al. [47], and research by Littunen et al. [19].

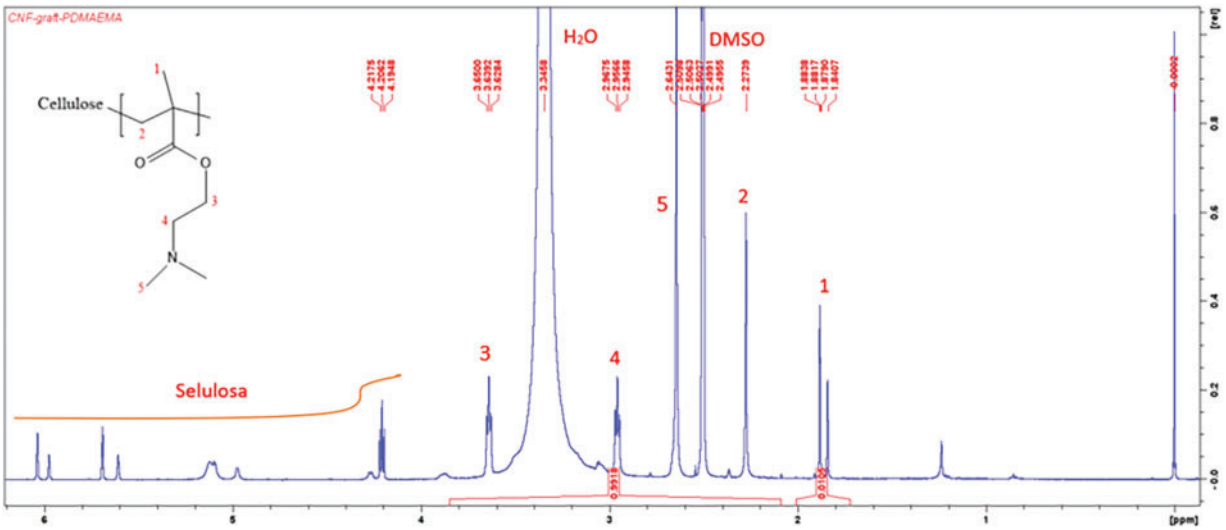

Figure 2: ^{1}H-NMR spectrum of CNF-g-PDMAEMA

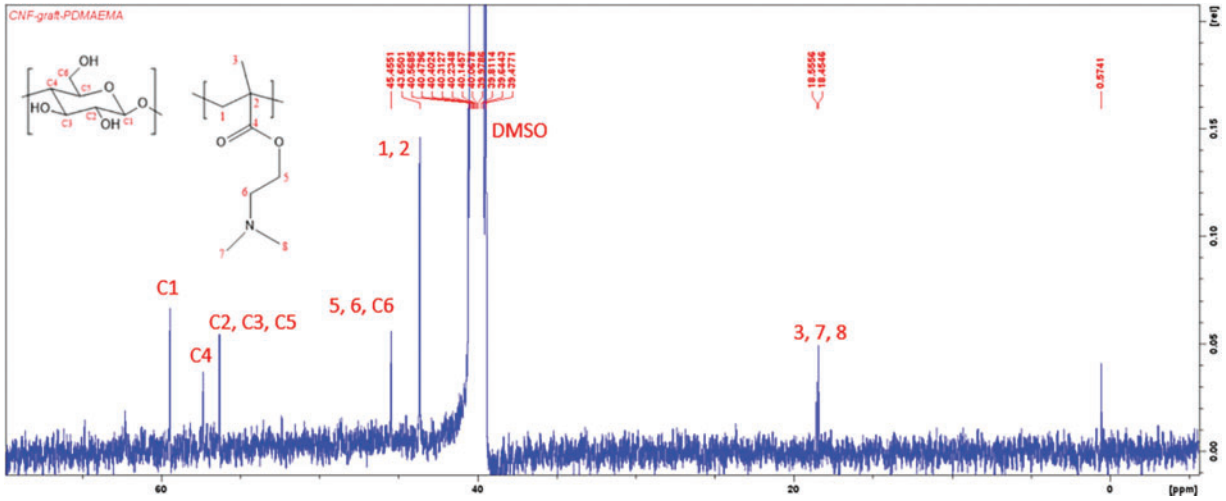

Figure 3: ^{13}C-NMR spectrum of CNF-g-PDMAEMA

NMR spectrum analysis denoted that the grafting process occurred as indicated by the presence of a peak of proton H_1 of DMAEMA on the ^{1}H-NMR spectrum and a peak of C_3 of DMAEMA on the ^{13}C-NMR spectrum. These peaks implied that DMAEMA experienced structure changes to PDMAEMA because the vinyl group did not appear on the ^{1}H-NMR and ^{13}C-NMR spectrum. Nevertheless, the structure of CNF-g-PDMAEMA produced still could not be estimated due to many peaks that overlap on the spectrum.

3.2.3 Degree of Grafting (DoG)

A study of the effect of reaction time, initiator concentration, and monomer amount on DoG was conducted to determine the optimal condition for the reaction to obtain the highest DoG. FTIR of graft copolymerization is shown in Fig. 4. Almost all reactions successfully produced graft copolymer except for CNF-g-PDMAEMA with reaction times of 30 and 60 min and CAN concentration of 3 mM. Increasing the polymerization time from 0 to 60 min for CNF-g-PHEMA caused an increase in the DoG (Fig. 5a). Longer polymerization time caused more graft copolymer to form because the initiator, monomer, and CNF could interact longer [48]. However, for CNF-g-PHEMA, DoG decreased from 90 to 120 min which might be caused by initiator concentration, monomer amount, and accessible free radical sites decreased along reaction time [49]. The highest DoG for CNF-g-PDMAEMA reached at 90 min and then decreased at 120 min (Fig. 5a). Therefore, the optimum reaction time for CNF-g-PDMAEMA was achieved at 90 and 60 min for CNF-g-PHEMA.

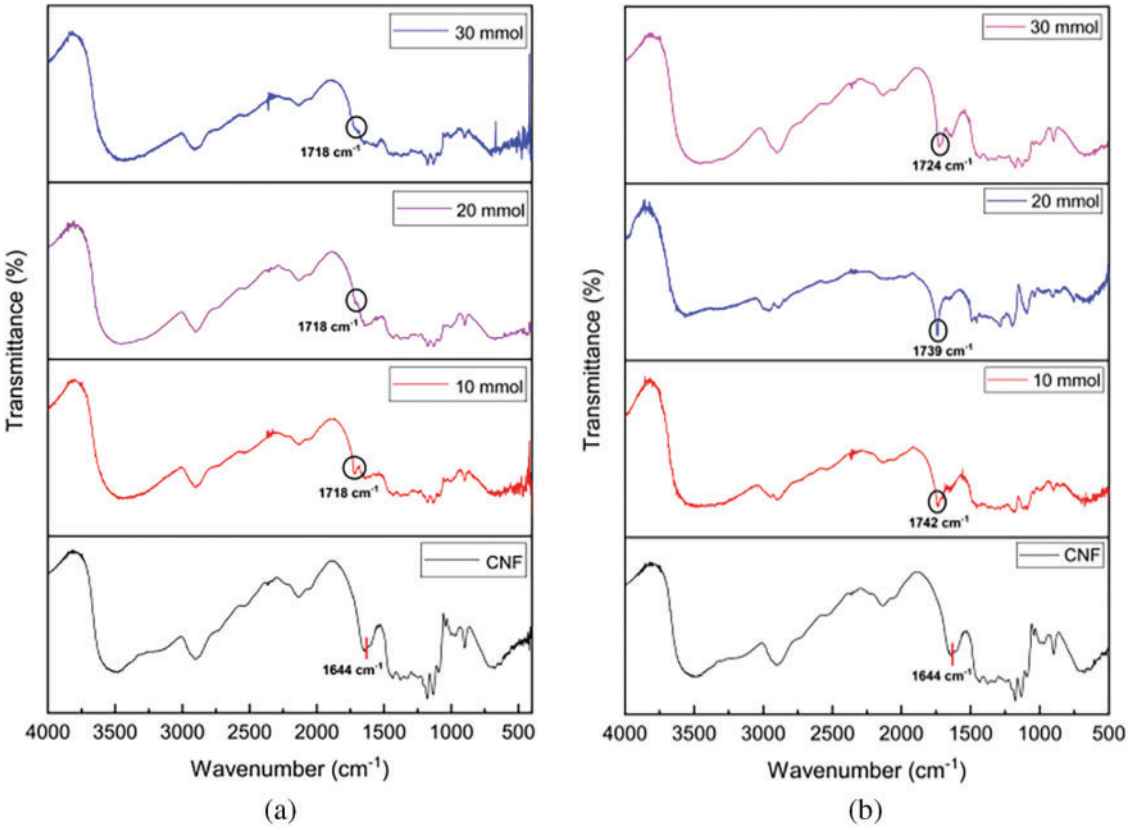

Figure 4: FTIR of **(a)** Monomer amount variation of CNF-g-PDMAEMA; **(b)** Monomer amount variation of CNF-g-PHEMA

The DoG increased as initiator concentration rose (Fig. 5b). A rise in initiator concentration caused more free radical sites to form, resulting in higher DoG. The initiator concentration of 7 mM produced eight times higher DoG than the initiator concentration of 5 mM for CNF-g-PDMAEMA. In comparison, for CNF-g-PHEMA, the DoG increased six times higher for an initiator concentration of 5 mM than the

initiator concentration of 1 mM. However, in general, the DoG of CNF-g-PHEMA was higher than CNF-g-PDMAEMA. The optimum initiator concentration was obtained in 7 mmol for CNF-g-PDMAEMA with the DoG value was 0.88% and 5 mmol for CNF-g-PHEMA had a DoG value of 6.32%.

The effect of monomer concentration on DoG was different between CNF-g-PDMAEMA and CNF-g-PHEMA. For CNF-g-PDMAEMA, the DoG tended to decrease as the monomer amount increased. This might be caused by higher amounts of DMAEMA monomers that increased the chance for homopolymer to form instead of graft copolymer. The highest DoG for CNF-g-PDMAEMA was 1.86% which was achieved at a DMAEMA amount of 10 mmol. On the contrary, the DoG value of CNF-g-PHEMA increased as the monomer amount increased because there could be more monomers ready to be grafted on free radical sites. The highest DoG for CNF-g-PHEMA was 10.09%, reached at a HEMA amount of 30 mmol (Fig. 5c).

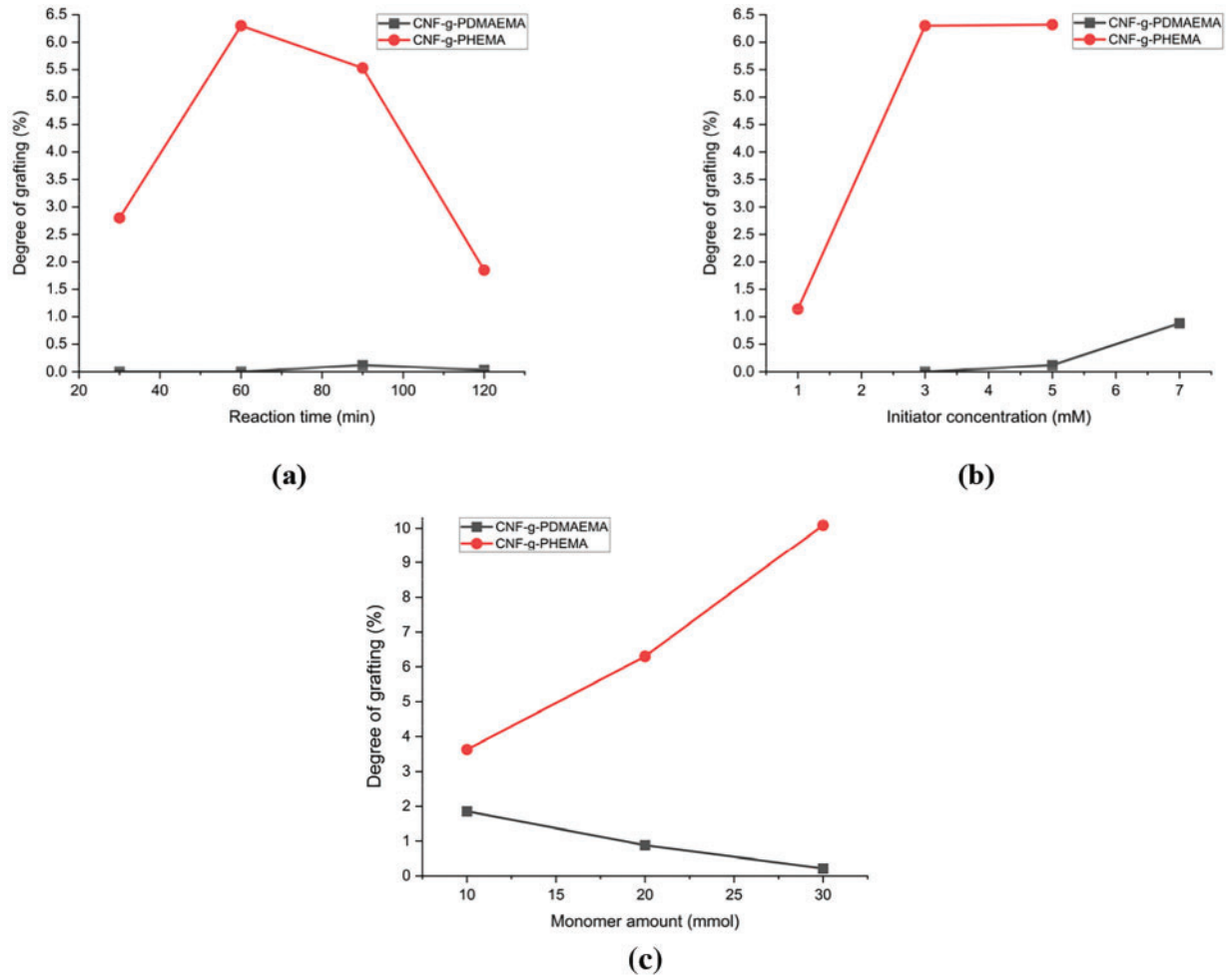

Figure 5: Degree of Grafting of CNF-g-PDMAEMA and CNF-g-PHEMA for **(a)** Reaction time variation; **(b)** Initiator concentration variation; **(c)** Monomer amount variation

3.2.4 XRD Characterization

XRD characterization was performed to determine the structure of CNF-g-PDMAEMA polymer chains. CNF-g-PDMAEMA had both amorphous and crystalline structures that could be seen by the

presence of diffraction peaks at 2θ around 16° that corresponded to the amorphous region and 22° which belonged to the crystalline structure of CNF [50]. On the other hand, PDMAEMA is known as a non-crystalline polymer due to its atactic structure, resulting in no special stereochemistry between its pendent groups and being unable to form a crystalline structure [51]. The XRD pattern of CNF-g-PDMAEMA is shown in Fig. 6.

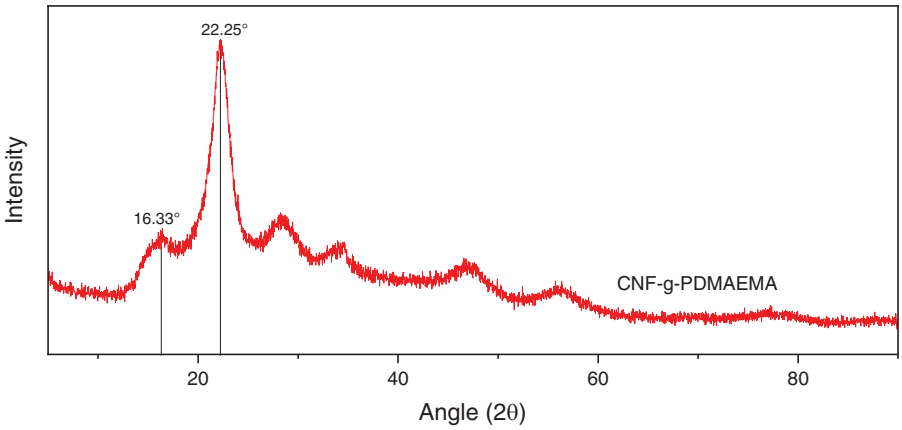

Figure 6: XRD Pattern of CNF-g-PDMAEMA

The polymer structure of CNF-g-PDMAEMA was determined by analyzing the crystallinity index (CI) based on the ratio of crystalline region area to the total area in the XRD diffraction pattern. The crystallinity index provides a quantitative measure of the orientation of the CNF crystals, with lower crystallinity indicating higher amorphous regions. The results of XRD data analysis showed that CNF-g-PDMAEMA, in this case CNF-g-PDMAEMA7, had a crystallinity of 17.05% and an amorphous content of 82.95%, explained that the lower crystallinity index caused by the structure of graft copolymers had a poor order of CNF crystals due to misorientation by the presence of the non-crystalline polymer PDMAEMA during the grafting process and disrupting the hydrogen bond between [52]. From the results, it can be concluded that the structure of CNF-g-PDMAEMA consisted of elongated chains of CNF that were aligned together with PDMAEMA, a non-crystalline polymer, and formed sandwich between the CNF chains.

3.2.5 Viscosity

In coating rheology, the resistance of a coating formulation to an applied flow is specifically measured as viscosity. In coating applications, viscosity affects the ease of the coating process since it affects the drainage rate, initial coating thickness, and ease of coating. If the viscosity is too low, coating will be difficult to do because the coating distribution is likely to be uneven and the high water content affects the drying and strength of the paper after drying. Meanwhile, if the viscosity is too high, penetration of the coating into the paper fibers is difficult so it will not increase the mechanical strength of the paper [53]. As displayed in Fig. 7, the viscosity of the grafted CNF increased along with the number of added monomers. The viscosity of CNF-g-PDMAEMA with a variation of DMAEMA moles of 10 mmol was 226 cP while CNF-g-PDMAEMA with a variation of DMAEMA moles of 30 mmol was 316 cP. The results were slightly different from CNF-g-PHEMA where with a HEMA amount of 10 mmol the viscosity was 300 cP while with a monomer amount of 30 mmol, the viscosity was 493.33 cP. Most probable the increase in viscosity occurred because of the increasing chain length of the grafted polymer chains that led to the rise of the molar masses, and thus, the viscosity rose, as described in the Mark-Howink equation [54]. Compared to CNF, CNF itself had a viscosity of 430 cP,

meaning that in general, the grafting reduced the viscosity of CNF. This phenomenon might occur because of the addition of branched polymer chains in the grafted CNF.

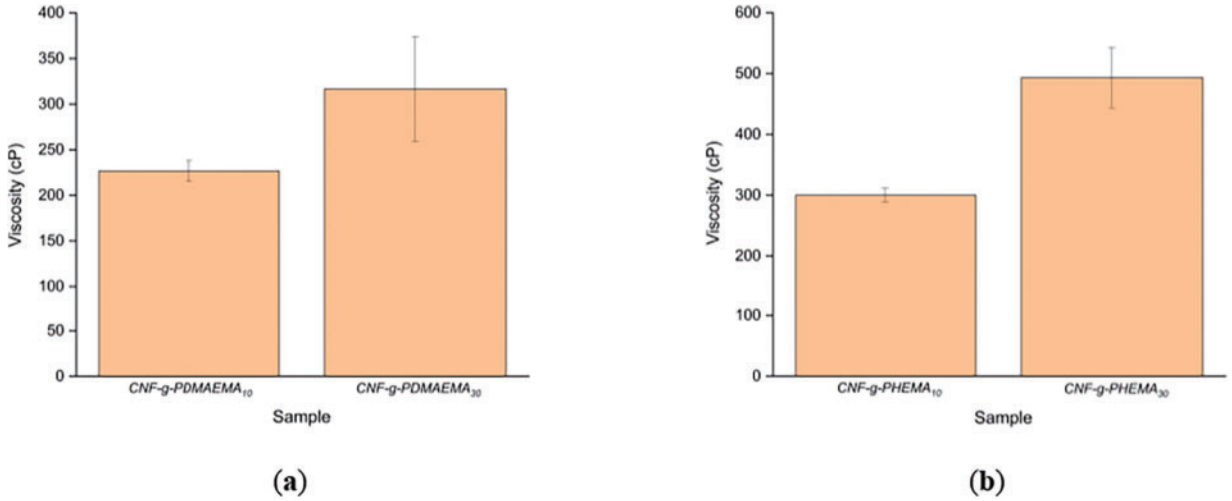

Figure 7: Viscosity of **(a)** CNF-g-PDMAEMA; **(b)** CNF-g-PHEMA

3.3 Performance of the Coated Paper

3.3.1 Water Absorption (Cobb$_{60}$ Method)

The Cobb$_{60}$ test was conducted to determine the water absorption capacity of the coated paper as shown in Fig. 8. The blank paper had the highest Cobb$_{60}$ of 27.74 g/m^2, while the Cobb$_{60}$ of paper coated with CNF-g-PDMAEMA was lower, at 24.60 and 26.8 g/m^2 and Cobb$_{60}$ of paper coated with CNF-g-PHEMA was also lower at 25.75 and 14.16 g/m^2. Paper coated with CNF-g-PDMAEMA with a DMAEMA mole variation of 10 mmol experienced a lower Cobb$_{60}$ than paper coated with CNF-g-PDMAEMA with a DMAEMA mole variation of 30 mmol. The DoG affected water absorption, as higher DoG led to the formation of a network that could retain water more effectively. CNF-g-PDMAEMA with a DMAEMA mole variation of 10 mmol had a higher DoG than the variation with 30 mmol, which resulted in paper coated with CNF-g-PDMAEMA (10 mmol) having better hydrophobic properties. Similarly, CNF-g-PHEMA with a HEMA variation of 30 mmol experienced a lower water absorption compared to CNF-g-PHEMA with a HEMA variation of 10 mmol. This decrease in water absorption indicated that paper had improved hydrophobicity [55]. The coating on the paper could cover its pores with the CNF graft layer, making it more difficult for water to be absorbed into the paper.

3.3.2 Water Contact Angle

The water contact angle of the coated paper was also studied, and the results are presented in Fig. 9. The blank paper was obtained with a contact angle of 78.20°, while the paper coated with CNF-g-PHEMA had a water contact angle of more than 90°. With the increase in the water contact angle, it can be stated that CNF-g-PHEMA experienced an increase in its hydrophobicity. Likewise, the water contact angle of CNF-g-PDMAEMA also increased with the increase in the size of the bar coater, reaching a maximum value of 92.58°. This might happen because the larger the size of the bar coater was, the thickness of the coating also increased. Increasing thickness causes the opportunity for the coating to cover the pore structure of the paper to increase, which affected the difficulty of water vapor and water penetrating the paper [56].

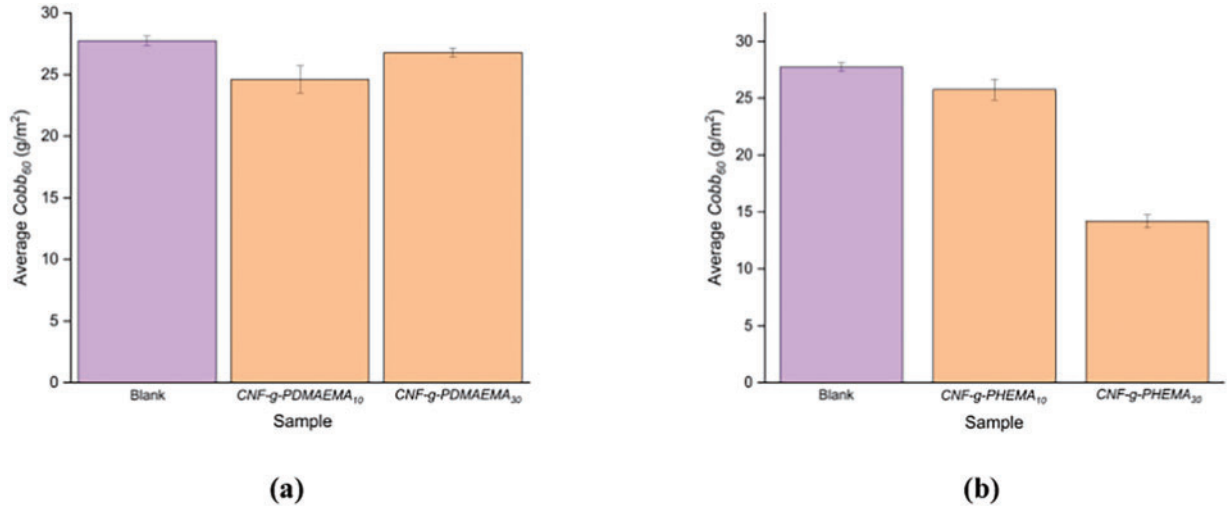

Figure 8: Water absorption test ($Cobb_{60}$) of the paper coated with **(a)** CNF-g-PDMAEMA; **(b)** CNF-g-PHEMA

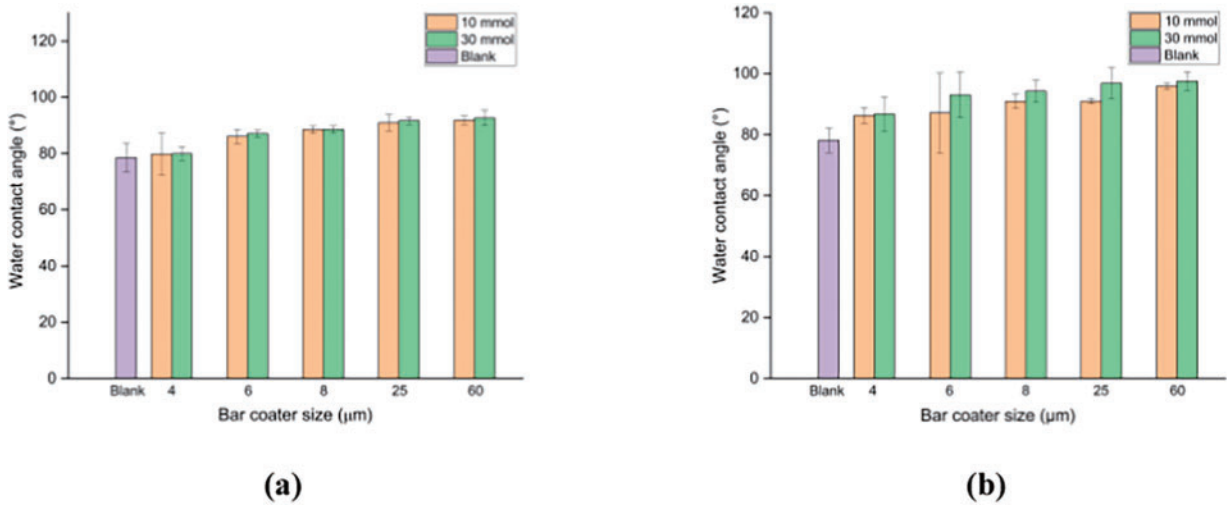

Figure 9: Water contact angle of the paper coated with **(a)** CNF-g-PDMAEMA; **(b)** CNF-g-PHEMA

3.3.3 Water Vapor Transmission Rate (WVTR)

The samples tested were blank paper, and CNF-g-PDMAEMA and CNF-g-PHEMA coated paper with 10 and 30 mmol of monomer, using various bar coater sizes. As shown in Fig. 10, the paper coated with all variations exhibited a decrease in WVTR value compared to the blank paper. In the paper coated with CNF-g-PDMAEMA, a more significant decrease in WVTR was observed with the 10 mmol DMAEMA mole variation compared to the 30 mmol variation. This phenomenon occurred because the DoG for the 10 mmol DMAEMA variation was higher than that of 30 mmol, allowing easier formation of entanglements. This network structure helped prevent water vapor from penetrating the paper [53]. Therefore, the CNF graft coating improved the water vapor barrier properties of the paper, as a lower WVTR value indicated less water vapor absorption.

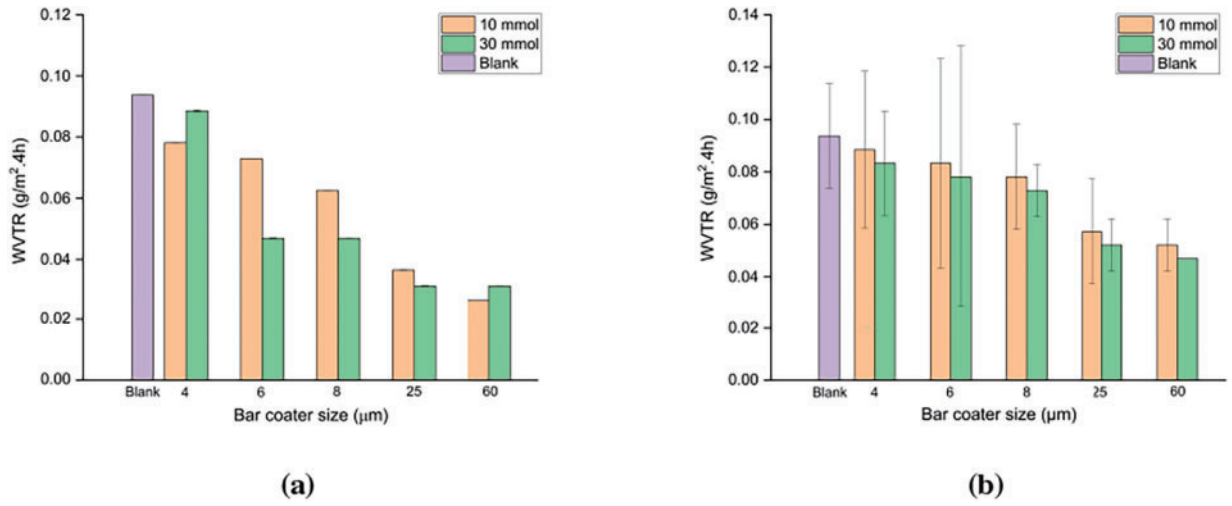

Figure 10: WVTR of the paper coated with **(a)** CNF-g-PDMAEMA; **(b)** CNF-g-PHEMA

3.3.4 Oil Absorption

The results of the oil absorption test were calculated based on the length of the absorbed oval shape of the oil on paper. In this test, two variations were carried out, namely testing in the direction of the fiber (machine direction/MD) and against the direction of the fiber (cross direction/CD). The test results in Fig. 11 show the oil absorption of paper coated with CNF-g-PDMAEMA and CNF-g-PHEMA. On paper coated with CNF-graft-PDMAEMA, the oil absorption value of the DMAEMA mole variation of 30 mmol for both machine direction and cross direction tests showed lower values than CNF-g-PDMAEMA DMAEMA mole variation of 10 mmol. This was slightly different from the results of paper coated with CNF-g-PHEMA, in which the one with the lower oil absorption value was paper coated with CNF-g-PHEMA variation of HEMA 10 mmol. Moreover, all coated papers had lower oil absorption values than blank paper. The pores of the paper filled with the coating made it difficult for oil to be absorbed into the paper, resulting in the oval shape being longer. Overall, lower oil absorption was obtained in the machine direction test compared to the cross direction.

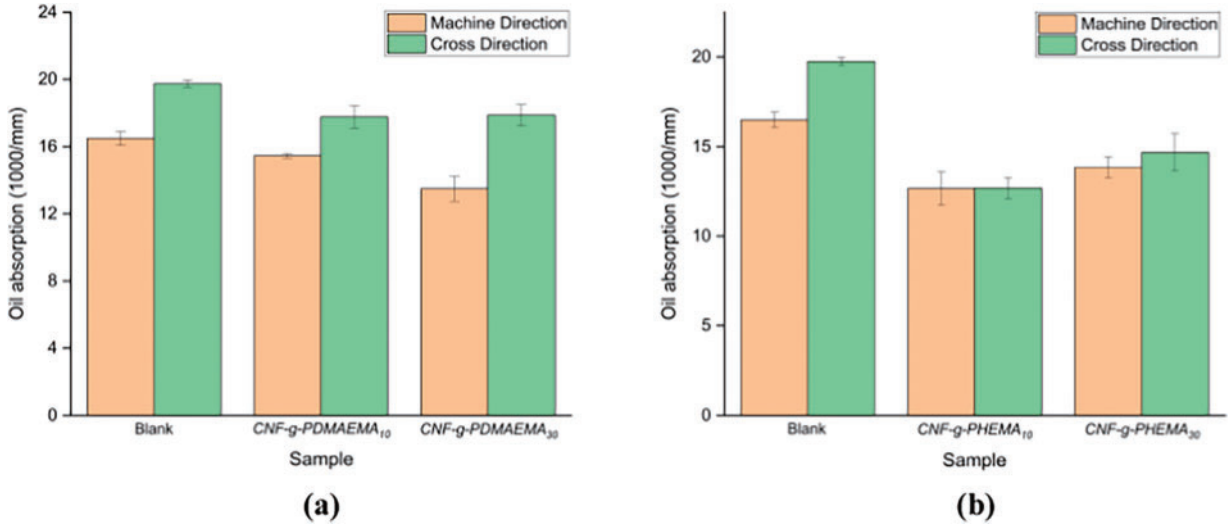

Figure 11: Oil absorption of the paper coated with **(a)** CNF-g-PDMAEMA; **(b)** CNF-g-PHEMA

3.3.5 Tensile Strength

Fig. 12 shows the results of the tensile strength test for the coated paper. Based on the data, there was an increase in tensile strength of 5% and 0.3% in paper samples coated with CNF-graft-PDMAEMA with DMAEMA mole variations of 10 and 30 mmol, respectively, compared to the blank paper. In the case of CNF-g-PHEMA, the paper with greater tensile strength was the one coated with CNF-g-PHEMA with a HEMA mole variation of 30 mmol. An increase of approximately 3% in tensile strength was observed in paper samples coated with CNF-g-PHEMA containing 30 mmol of HEMA, compared to the blank paper. This increase in tensile strength could be due to the filling of gaps between the fibers and the polymer. CNF could enhance the tensile strength of paper because of the potential bonding that results from the intertwining of nanofibers in the matrix, forming a continuous network [53]. Additionally, there was a possibility of cross-covalent bond formation between CNF and the acrylate polymer [53]. Previous work by Yang et al. [57] also mentioned that tensile strength of cellulose graft with acrylic monomers increased compared to the only monomer without cellulose.

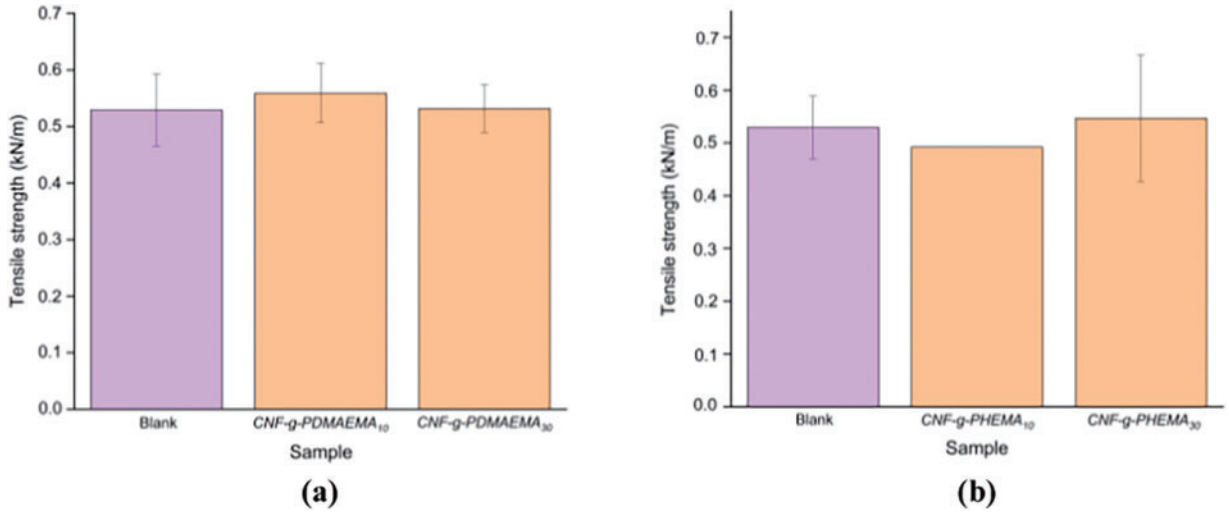

Figure 12: Tensile strength of the paper coated with **(a)** CNF-g-PDMAEMA; **(b)** CNF-g-PHEMA

4 Conclusions

In this work, we reported the modification of CNF to enhance the barrier properties of CNF on paper coating applications. Grafting CNF with DMAEMA or HEMA was done successfully using redox-initiated free radical polymerization. FTIR was used to confirm graft copolymerization of DMAEMA or HEMA to CNF. The DoG increased with an increase in reaction time and then decreased when there were no more active sites available for polymerization. Furthermore, an increase in DoG achieved at higher initiator concentration was caused by more free radical sites that were available to encourage graft copolymerization. The two effects mentioned before were linear for CNF-g-PDMAEMA and CNF-g-PHEMA. However, the effect of the monomer amounts experienced different trend, that was, increasing DoG as decreasing monomer amount for CNF-g-PDMAEMA and increasing DoG as increasing monomer amount for CNF-g-PHEMA. Notably, the viscosity of the grafted CNF was found to be in the acceptable number for coating application. This study revealed that paper coated with CNF-g-PHEMA and CNF-g-PDMAEMA showed an increase in water contact angle, reaching an angle of 97.51° and 92.58°, respectively, while the corresponding $Cobb_{60}$ values decreased by 49% and 11%. Compared to the blank paper, the oil absorption for both coated

papers likewise reduced. Paper coated with CNF-g-PHEMA showed a 3% improvement in tensile strength, whereas paper coated with CNF-g-PDMAEMA showed a 5% increase in mechanical characteristics. These results concluded that coating paper with CNF-g-PDMAEMA and CNF-g-PHEMA successfully improved the mechanical properties, hydrophobicity, and oleophobicity of paper. It is worth noting that the grafting procedure could be modified to improve the mechanical and barrier properties of the coated paper which might further widen the use of modified CNF in paper-based food packaging.

Acknowledgement: The authors acknowledge Kementerian Pendidikan, Kebudayaan, Riset dan Teknologi, for the research funding of Hibah Penelitian Fundamental Reguler under funding year of 2024. The authors acknowledge the Integrated Laboratory and Research Center (ILRC) Universitas Indonesia, Badan Riset Inovasi Nasional (BRIN), and Laboratorium Pengujian Bahan Grafika Politeknik Negeri Media Kreatif Jakarta for the characterization facilities. Noteworthy, the authors thank Annisa Nurul Syabila from Department of Chemical Engineering, Institut Teknologi Indonesia for her assistance in preparing this article.

Funding Statement: This work was supported by Hibah Penelitian Fundamental Reguler Kementerian Pendidikan, Kebudayaan, Riset dan Teknologi under funding year of 2024 with contract number: 051/E5/PG.02.00.PL/2024; NKB-903/UN2.RST/HKP.05.00/2024.

Author Contributions: Noverra Mardhatillah Nizardo contributed to conceptualizing the research, data analysis, and interpretation, reviewing and editing the original draft, and funding acquisition. Alifah Nurul Saffanah and Annisa Fitri Salsabila conducted experiments, characterized the products, and wrote the original draft of the manuscript. Amanda Aurellia Putri edited the original draft and prepared the graphical abstract. Aniek Sri Handayani designed the methodology for coating and performance tests and data interpretation and reviewed and edited the original draft. Azizah Intan Pangesty and Mochamad Chalid reviewed and edited the original draft. All authors reviewed the results and approved the final version of the manuscript.

Availability of Data and Materials: The authors confirm that the data supporting the findings of this study are available within the article.

Ethics Approval: Not applicable.

Conflicts of Interest: The authors declare no conflicts of interest to report regarding the present study.

References

1. Roesfitawati. Desain kemasan produk makanan olahan. Kementerian perdagangan republik Indonesia [Internet]. [cited 2024 Oct 24] (In Indonesian). Available from: http://djpen.kemendag.go.id.
2. Nugrahaeni M. Kemasan pangan. 1st ed. Yogyakarta: Plantaxia. 2018; p.3–4.
3. Moore CJ. Synthetic polymers in the marine environment: a rapidly increasing, long-term threat. Environ Res. 2008;108(2):131–9. doi:10.1016/j.envres.2008.07.025.
4. Khoaele KK, Gbadeyan OJ, Chunilall V, Sithole B. The devastation of waste plastic on the environment and remediation processes: a critical review. Sustainability. 2023;15(6):5233. doi:10.3390/su15065233.
5. Geyer R, Jambeck JR, Law KL. Production, use, and fate of all plastics ever made. Sci Adv. 2017;3(7):e1700782. doi:10.1126/sciadv.1700782.
6. Smith AM, Moxon S, Morris GA. Biopolymers as wound healing materials. In: Ågren MS, editor. Wound healing biomaterials. Amsterdam, The Netherlands: Elsevier; 2016. p. 261–87. doi:10.1016/b978-1-78242-456-7.00013-1.
7. Hassan B, Chatha SAS, Hussain AI, Zia KM, Akhtar N. Recent advances on polysaccharides, lipids and protein based edible films and coatings: a review. Int J Biol Macromol. 2018;109(4):1095–107. doi:10.1016/j.ijbiomac.2017.11.097.
8. Liu X, Qin Z, Ma Y, Liu H, Wang X. Cellulose-based films for food packaging applications: review of preparation, properties, and prospects. J Renew Mater. 2023;11(8):3203–25. doi:10.32604/jrm.2023.027613.

9. Reshmy R, Philip E, Paul SA, Madhavan A, Sindhu R, Binod P, et al. Nanocellulose-based products for sustainable applications-recent trends and possibilities. Rev Environ Sci Bio Technol. 2020;19(4):779–806. doi:10.1007/s11157-020-09551-z.
10. Liu W, Liu H, Liu K, Du H, Liu Y, Si C. Paper-based products as promising substitutes for plastics in the context of bans on non-biodegradables. BioResources. 2020;15(4):7309–12. doi:10.15376/biores.15.4.7309-7312.
11. Huang J, Ma X, Yang G, Alain D. Introduction to nanocellulose. In: Huang J, Dufresne A, Lin N, editors. Nanocellulose. Hoboken, NJ, USA: John Wiley & Sons, Inc. 2019. p. 1–20.
12. Rol F, Belgacem MN, Gandini A, Bras J. Recent advances in surface-modified cellulose nanofibrils. Prog Polym Sci. 2019;88(658):241–64. doi:10.1016/j.progpolymsci.2018.09.002.
13. Raj P, Batchelor W, Blanco A, de la Fuente E, Negro C, Garnier G. Effect of polyelectrolyte morphology and adsorption on the mechanism of nanocellulose flocculation. J Colloid Interface Sci. 2016;481(2):158–67. doi:10.1016/j.jcis.2016.07.048.
14. Olszewska A, Junka K, Nordgren N, Laine J, Rutland MW, Österberg M. Non-ionic assembly of nanofibrillated cellulose and polyethylene glycol grafted carboxymethyl cellulose and the effect of aqueous lubrication in nanocomposite formation. Soft Matter. 2013;9(31):7448. doi:10.1039/c3sm50578b.
15. Ratnawati, Septevani AA, Nurul A, Arifin Y, Handayani AS. Synthesis and characterization of cellulose nanofiber/poly-vinyl alcohol (CNF/PVA) nanocomposites for gas barrier applications in paper packaging. Mater Today Proc. 2023. doi:10.1016/j.matpr.2023.04.248.
16. Nizardo NM, Sugandi NAD, Handayani AS. Poly(vinyl alcohol)/carboxymethyl cellulose/cellulose nanofibrils nanocomposite as coating for food packaging paper. Polym Plast Technol Mater. 2024;63(5):447–58. doi:10.1080/25740881.2023.2291435.
17. Fujisawa S, Zhang J, Saito T, Iwata T, Isogai A. Cellulose nanofibrils as templates for the design of poly(l-lactide)-nucleating surfaces. Polymer. 2014;55(13):2937–42. doi:10.1016/j.polymer.2014.04.019.
18. Liyanage S, Acharya S, Parajuli P, Shamshina JL, Abidi N. Production and surface modification of cellulose bioproducts. Polymers. 2021;13(19):3433. doi:10.3390/polym13193433.
19. Littunen K, Hippi U, Johansson LS, Österberg M, Tammelin T, Laine J, et al. Free radical graft copolymerization of nanofibrillated cellulose with acrylic monomers. Carbohydr Polym. 2011;84(3):1039–47. doi:10.1016/j.carbpol.2010.12.064.
20. Kedzior SA, Graham L, Moorlag C, Dooley BM, Cranston ED. Poly(methyl methacrylate)-grafted cellulose nanocrystals: one-step synthesis, nanocomposite preparation, and characterization. Can J Chem Eng. 2016;94(5):811–22. doi:10.1002/cjce.22456.
21. Hollertz R, Durán VL, Larsson PA, Wågberg L. Chemically modified cellulose micro- and nanofibrils as paper-strength additives. Cellulose. 2017;24(9):3883–99. doi:10.1007/s10570-017-1387-6.
22. Boufi S, González I, Delgado-Aguilar M, Tarrès Q, Àngels Pèlach M, Mutjé P. Nanofibrillated cellulose as an additive in papermaking process: a review. Carbohydr Polym. 2016;154(2):151–66. doi:10.1016/j.carbpol.2016.07.117.
23. Aulin C, Ström G. Multilayered alkyd resin/nanocellulose coatings for use in renewable packaging solutions with a high level of moisture resistance. Ind Eng Chem Res. 2013;52(7):2582–9. doi:10.1021/ie301785a.
24. Missoum K, Belgacem MN, Bras J. Nanofibrillated cellulose surface modification: a review. Materials. 2013;6(5):1745–66. doi:10.3390/ma6051745.
25. Brodin FW, Gregersen ØW, Syverud K. Cellulose nanofibrils: challenges and possibilities as a paper additive or coating material—a review. Nord Pulp Pap Res J. 2014;29(1):156–66. doi:10.3183/npprj-2014-29-01-p156-166.
26. Garcia-Valdez O, Brescacin T, Arredondo J, Bouchard J, Jessop PG, Champagne P, et al. Grafting CO_2-responsive polymers from cellulose nanocrystals via nitroxide-mediated polymerisation. Polym Chem. 2017;8(28):4124–31. doi:10.1039/c7py00631d.
27. Rasheed M, Parveez B. Coating on packaging products to enhance shelf life. In: Saba N, Jawaid M, Thariq M, editors. Biopolymers and biocomposites from agro-waste for packaging applications. Amsterdam, The Netherlands: Elsevier; 2021. p. 1–33. doi:10.1016/b978-0-12-819953-4.00012-4.
28. Wu F, Misra M, Mohanty AK. Challenges and new opportunities on barrier performance of biodegradable polymers for sustainable packaging. Prog Polym Sci. 2021;117(11):101395. doi:10.1016/j.progpolymsci.2021.101395.

29. Rastogi V, Samyn P. Bio-based coatings for paper applications. Coatings. 2015;5(4):887–930. doi:10.3390/coatings5040887.
30. Jahangiri F, Mohanty AK, Pal AK, Shankar S, Rodriguez-Uribe A, Clemmer R, et al. PHBV coating on biodegradable plastic sheet: effect of coating on morphological, mechanical and barrier properties. Prog Org Coat. 2024;189:108270. doi:10.1016/j.porgcoat.2024.108270.
31. Septevani AA, Burhani D, Sudiyarmanto S. Pengaruh proses pemutihan multi tahap serat selulosa Dari limbah tandan kosong kelapa sawit. J Kimia Kemasan. 2018;40(2):71 (In Indonesian). doi:10.24817/jkk.v40i2.3508.
32. Segal L, Creely JJ, Martin AE, Conrad CM. An empirical method for estimating the degree of crystallinity of native cellulose using the X-ray diffractometer. Text Res J. 1959;29(10):786–94. doi:10.1177/004051755902901003.
33. Dewanti DP. Potensi selulosa Dari limbah tandan kosong kelapa sawit untuk bahan Baku bioplastik ramah lingkungan. Jurtekling. 2018;19(1):81 (In Indonesian). doi:10.29122/jtl.v19i1.2644.
34. Susi S, Ainuri M, Wagiman W, Falah MAF. Characterization and selection of microcrystalline cellulose from oil palm empty fruit bunches for strengthening hydrogel films. J Renew Mater. 2024;12(3):513–37. doi:10.32604/jrm.2024.045586.
35. Tan JY, Tey WY, Panpranot J, Lim S, Lee KM. Valorization of oil palm empty fruit bunch for cellulose fibers: a reinforcement material in polyvinyl alcohol biocomposites for its application as detergent capsules. Sustainability. 2022;14(18):11446. doi:10.3390/su141811446.
36. Yimlamai B, Choorit W, Chisti Y, Prasertsan P. Cellulose from oil palm empty fruit bunch fiber and its conversion to carboxymethylcellulose. J Chem Technol Biotechnol. 2021;96(6):1656–66. doi:10.1002/jctb.6689.
37. Chieng BW, Lee SH, Ibrahim NA, Then YY, Loo YY. Isolation and characterization of cellulose nanocrystals from oil palm mesocarp fiber. Polymers. 2017;9(8):355. doi:10.3390/polym9080355.
38. Susi S, Ainuri M, Wagiman W, Falah MAF. High-yield alpha-cellulose from oil palm empty fruit bunches by optimizing thermochemical delignification processes for use as microcrystalline cellulose. Int J Biomater. 2023;2023(6):9169431. doi:10.1155/2023/9169431.
39. Bekele AE, Lemu HG, Jiru MG. Experimental study of physical, chemical and mechanical properties of enset and sisal fibers. Polym Test. 2022;106(3):107453. doi:10.1016/j.polymertesting.2021.107453.
40. Ye H, Zhang Y, Yu Z, Mu J. Effects of cellulose, hemicellulose, and lignin on the morphology and mechanical properties of metakaolin-based geopolymer. Constr Build Mater. 2018;173:10–6. doi:10.1016/j.conbuildmat.2018.04.028.
41. Feleke K, Thothadri G, Beri Tufa H, Rajhi AA, Ahmed GMS. Extraction and characterization of fiber and cellulose from Ethiopian linseed straw: determination of retting period and optimization of multi-step alkaline peroxide process. Polymers. 2023;15(2):469. doi:10.3390/polym15020469.
42. Radakisnin R, Abdul Majid MS, Jamir MRM, Jawaid M, Sultan MTH, Mat Tahir MF. Structural, morphological and thermal properties of cellulose nanofibers from Napier fiber (*Pennisetum purpureum*). Materials. 2020;13(18):4125. doi:10.3390/ma13184125.
43. Blažic R, Kučić Grgić D, Kraljić Roković M, Vidović E. Cellulose-g-poly(2-(dimethylamino)ethylmethacrylate) hydrogels: synthesis, characterization, antibacterial testing and polymer electrolyte application. Gels. 2022;8(10):636. doi:10.3390/gels8100636.
44. Credou J, Faddoul R, Berthelot T. One-step and eco-friendly modification of cellulose membranes by polymer grafting. RSC Adv. 2014;4(105):60959–69. doi:10.1039/c4ra11219a.
45. Liu X, Yin H, Song X, Zhang Z, Li J. Lignin-based nonviral gene carriers functionalized by poly[2-(dimethylamino)ethyl methacrylate]: effect of grafting degree and cationic chain length on transfection efficiency. Biomolecules. 2022;12(1):102. doi:10.3390/biom12010102.
46. Neelamegan H, Yang DK, Lee GJ, Anandan S, Sorrentino A, Wu JJ. Synthesis of magnetite-based polymers as mercury and anion sensors using single electron transfer-living radical polymerization. ACS Omega. 2020;5(13):7201–10. doi:10.1021/acsomega.9b03653.
47. Okushita K, Komatsu T, Chikayama E, Kikuchi J. Statistical approach for solid-state NMR spectra of cellulose derived from a series of variable parameters. Polym J. 2012;44(8):895–900. doi:10.1038/pj.2012.82.

48. Rosli NA, Ahmad I, Abdullah I, Anuar FH, Mohamed F. Hydrophobic modification of cellulose isolated from *Agave angustifolia* fibre by graft copolymerisation using methyl methacrylate. Carbohydr Polym. 2015;125:69–75. doi:10.1016/j.carbpol.2015.03.002.
49. Joshi JM, Sinha VK. Ceric ammonium nitrate induced grafting of polyacrylamide onto carboxymethyl chitosan. Carbohydr Polym. 2007;67(3):427–35. doi:10.1016/j.carbpol.2006.06.021.
50. Wulan PPDK, Ismojo, Khumaeroh, Syabila AN, Handayani AS, Ratnawati. Sustainable extraction of cellulose nanocrystals from empty palm oil bunches via low-acid hydrolysis. Results Eng. 2024;24(5):103012. doi:10.1016/j.rineng.2024.103012.
51. Odian G. Principles of polymerization. 3rd ed. Hoboken, NJ, USA: John Wiley & Sons, Inc. 1991. 27 p.
52. Kaith BS, Kalia S. A study of crystallinity of graft copolymers of flax fiber with binary vinyl monomers. e-Polymers. 2008;8(1):002. doi:10.1515/epoly.2008.8.1.11.
53. Hassan ML, Fadel SM, Hassan EA. Acrylate/nanofibrillated cellulose nanocomposites and their use for paper coating. J Nanomater. 2018;2018(9):4953834–10. doi:10.1155/2018/4953834.
54. Cowie JMG, Arrighi V. Polymers: chemistry and physics of modern materials. Boca Raton, FL, USA: CRC Press; 2007. 520 p. doi:10.1201/9781420009873.
55. Kunam PK, Ramakanth D, Akhila K, Gaikwad KK. Bio-based materials for barrier coatings on paper packaging. Biomass Convers Biorefin. 2022;14(12):1–16. doi:10.1007/s13399-022-03241-2.
56. Song Z, Xiao H, Zhao Y. Hydrophobic-modified nano-cellulose fiber/PLA biodegradable composites for lowering water vapor transmission rate (WVTR) of paper. Carbohydr Polym. 2014;111:442–8. doi:10.1016/j.carbpol.2014.04.049.
57. Yang W, Dominici F, Fortunati E, Kenny JM, Puglia D. Melt free radical grafting of glycidyl methacrylate (GMA) onto fully biodegradable poly(lactic) acid films: effect of cellulose nanocrystals and a masterbatch process. RSC Adv. 2015;5(41):32350–7. doi:10.1039/c5ra00894h.